Wozniak Matthew, Christopher (Orcid ID: 0000-0003-4434-2064)
Steiner Allison, L. (Orcid ID: 0000-0002-3823-1512)

Pollen rupture and its impact on precipitation in clean continental conditions

M. C. Wozniak[1], F. Solmon[2], and A. L. Steiner[1]

[1]Department of Climate and Space Sciences and Engineering, University of Michigan, Ann Arbor, MI 48109-2143

[2] Laboratoire D'Aerologie, Observatoire Midi-Pyrénées, Toulouse, France

Corresponding author: Matthew Wozniak (mcwoz@umich.edu)

Key Points:

- The first model of moisture-induced pollen rupture and release of subpollen particles (SPPs) is coupled to a regional climate model.
- During peak pollen season in the United States, simulated SPPs range from 1 to 1,000 cm^{-3}, depending on the number produced per pollen grain ruptured.
- SPP may have the ability to suppress precipitation regionally in clean continental CCN conditions and induce a negative feedback to SPP production.

Key words: biological aerosols, CCN, precipitation

This is the author manuscript accepted for publication and has undergone full peer review but has not been through the copyediting, typesetting, pagination and proofreading process, which may lead to differences between this version and the Version of Record. Please cite this article as doi: 10.1029/2018GL077692

Abstract

Pollen grains emitted from vegetation can rupture, releasing subpollen particles (SPPs) as fine atmospheric particulates. Previous laboratory research demonstrates potential for SPPs as efficient cloud condensation nuclei (CCN). We develop the first model of atmospheric pollen grain rupture, and implement the mechanism in regional climate model simulations over spring pollen season in the United States with a CCN-dependent moisture scheme. The source of SPPs (surface or in-atmosphere) depends on region and sometimes season, due to the distribution of relative humidity and rain. Simulated concentrations of SPPs are approximately 1-10 or 1-1,000 cm^{-3}, depending on the number of SPPs produced per pollen grain (n_{spg}). Lower n_{spg} (10^3) produces a negligible effect on precipitation, but high n_{spg} (10^6) in clean continental CCN background concentrations (100 CCN cm^{-3}) shows SPPs suppress average seasonal precipitation by 32% and shift rates from heavy to light while increasing dry days. This effect is smaller (2% reduction) for polluted air.

Plain Language Summary

Pollen grains emitted by wind from a variety of plants can swell from exposure to high levels of humidity, creating internal pressure that may cause the grains to rupture. Particles that are ten to a thousand times smaller than pollen grains are released in the process. These subpollen particles (SPPs) have been found in laboratory studies to efficiently collect water on their surfaces, making them potential cloud condensation nuclei (CCN, i.e. particles that may grow into cloud droplets). We have developed a numerical model of pollen rupture that interfaces with an atmosphere model to determine 1) how many SPPs are produced during the pollen season from two different sources: rupture of pollen at the surface and rupture of airborne pollen grains; 2) the geographic and vertical distribution of SPPs seasonally; and 3) the impact of SPPs on regional precipitation. We find that the strength of either source in any region or phase of season depends on rain and relative humidity. We also find that SPPs have the potential to suppress seasonal precipitation in clean conditions when anthropogenic pollution is not present depending on how many are released for each pollen grain that ruptures. The magnitude of suppression regionally is dependent on source magnitude of SPPs, as well as the availability of water vapor.

1 Introduction

Aerosol particles can affect Earth's climate by their interactions with clouds and radiation (Boucher et al., 2013). Depending on size and composition, some aerosol particles act as cloud condensation nuclei (CCN) and facilitate growth of cloud droplets (Fitzgerald, 1973). Changes to the number of CCN drive the first aerosol indirect effect,

also known as the Twomey effect or the cloud albedo effect which affects the reflectivity of clouds (Twomey, 1991), and the second aerosol indirect effect known as the cloud lifetime effect that influences precipitation (Albrecht, 1989). In the second indirect effect, increases in cloud-active aerosol lengthen cloud lifetime, which over time increases fractional cloudiness and global albedo. This not only affects the Earth's radiation budget but alters the rate, amount and/or spatial distribution of precipitation (Stevens & Feingold, 2009). Currently, the uncertainty range in the radiative forcing due to cloud adjustments by aerosols is -1.20 to 0.00 W m^{-2} (Stocker et al., 2013), including uncertainties due to both natural and anthropogenic aerosol properties as well as model representations of aerosol indirect effects (Regayre et al., 2014). The lack of constraints on the emissions and distribution of natural aerosols is particularly important to identifying the present-day natural and pre-industrial aerosol burdens, which both influence radiative forcing calculations (Carslaw et al. 2013; Carslaw et al. 2017).

Natural aerosol sources include primary emissions from the Earth's surface (e.g., mineral dust, sea salt from sea spray, and biological particles), as well as secondary particles that form in the atmosphere (e.g., sulfate from marine emissions, secondary organic aerosol). Primary biological aerosol particles (PBAPs) include bacteria and cellular material, fungi, plant fragments, decayed organic matter, pollen and spores (Després et al. 2012). Although several PBAPs have been identified as potential CCN (Ariya et al., 2009; Sun & Ariya, 2006), the exact contribution of PBAP to CCN numbers is yet to be constrained. Specifically among these different categories of PBAP, anemophilous or wind-driven pollen has been identified as a potential natural source of CCN (Griffiths et al., 2012), ice nucleating particles (INP) (Diehl, Quick, Matthias-Maser, Mitra, & Jaenicke, 2001), and giant CCN (Pope, 2010). While pollen grains may not contribute substantially to global CCN concentrations at ambient concentrations of 10-10^3 grains m^{-3} (Despres et al., 2012), there is growing evidence that regional counts may be higher (10^4 grains m^{-3}) and pollen grains may be transported farther than previously thought (Williams & Després, 2017).

In addition to direct emissions of pollen, the rupture of pollen and subsequent release of fine particles may contribute more substantially to CCN. Fresh pollen grains can rupture under moist conditions, such as during precipitation events (Grote et al. 2001; Grote et al. 2003) and high humidity (Taylor, Flagan, Miguel, Valenta, & Glovsky, 2004; Taylor, Flagan, Valenta, & Glovsky, 2002). They may also mechanically rupture under turbulent conditions by impact forces (Visez et al., 2015). When pollen grains rupture, they release cytoplasmic fragments known as subpollen particles (SPPs), which range in size from several nanometers to about one micron (Taylor et al., 2004). Rupture could occur on open anthers (i.e. at the surface) and SPPs can be subsequently dispersed to the atmosphere by disturbances like wind in dry conditions following rupture (Taylor et al., 2004). Rupture processes also may occur in the atmosphere, potentially in clouds or under high relative humidity (RH) conditions. SPPs likely have source regions similar to

pollen, though regional transport and weather patterns may facilitate the transport of these smaller particles and lead to longer atmospheric residence time. While there is some evidence of pollen fragments in ambient aerosol using indirect methods such as chemical tracers (Rathnayake et al., 2017) or biofluorescence (Perring et al., 2014), little is known about the temporal and spatial distribution of SPPs. Recently, it has been discovered that SPPs in the Aitken (<0.1 μm) and accumulation (0.1-2.5 μm) modes are efficient CCN (Steiner et al., 2015). While a positive "bioprecipitation" feedback has been proposed for biological ice nuclei (Morris et al., 2014), we hypothesize that moisture-dependent, CCN-active SPPs may be involved in a negative feedback mechanism between SPP production and precipitation due to sufficient CCN in the atmosphere.

2 Model simulations

We develop the first model to simulate pollen rupture in the Earth system and its influence on clouds and precipitation (Figure 1; Text S1). The rupture model is based on the moisture-induced rupture phenomenon observed in the laboratory (Grote et al. 2003; Grote et al. 2001; Taylor et al. 2004; Taylor et al. 2002), and estimates the release of SPPs from rupture of pollen grains at the surface (surface rupture) and aloft in the atmosphere (airborne rupture) (Figure 1). We implement the rupture mechanism in a regional climate model (RegCM4; Giorgi et al. 2012) to study the distribution of SPPs and impact on precipitation. By linking airborne SPPs to CCN concentrations in parameterizations of the second aerosol indirect effect (AIE) in the large-scale and convective moisture schemes, we simulate the sensitivity of precipitation to SPPs during the spring pollen season (March – June 2002) in the continental United States when pollen emissions are at their annual maximum. One large uncertainty is the number of SPPs released per ruptured pollen grain (n_{spg}). Here we compare 10-member ensemble simulations using two different SPP production rates. The first ensemble uses n_{spg} = 1,000 SPPs grain^{-1} (SPP_LIT, literature-derived value; Suphioglu et al. 1992). In the second ensemble, we calculate the total number of SPPs produced if all pollen grain mass converted to SPPs, yielding $n_{spg} = 3.06\times10^{6}$ SPPs grain^{-1} (see Text S1 for calculation). Realistically, not all pollen mass can become SPPs (e.g. intact pollen shell), so we round to the nearest order of magnitude or n_{spg} = 1,000,000 SPPs grain^{-1} (SPP_HIGH), providing an upper limit to n_{spg}. Both of these simulations add SPP to a clean continental background CCN of 100 CCN cm^{-3} and are compared to an ensemble with background CCN, only.

The use of the 100 CCN cm^{-3} background is based on estimates for the pre-industrial continental conditions (Carslaw et al. 2017) and present-day observations of clean conditions globally (200±90 cm^{-3} CCN at 0.4% supersaturation, $CCN_{0.4}$; Andreae, 2009). Recent measurements of clean continental conditions at Storm Peak Lab in Colorado observe a mean spring CCN concentration of 218 (±119) CCN cm^{-3} (Salwen et

al., 2010), close to our selected background concentration. Moreover, despite upwind anthropogenic pollution from urban areas and power plants, long-term measurements from 1998-2016 of condensation nuclei (CN) in the free troposphere at Storm Peak Lab show an average spring CN concentration of about 1,202 (± 151) CN cm^{-3}, corresponding to 132-168 $CCN_{0.6}$ cm^{-3} using $CCN_{0.6}$/CN ratios of 0.11-0.14 measured at Storm Peak (Samy et al., 2010) for a supersaturation of 0.6%, thus supporting our selection A synthesis of global polluted conditions conditions suggests higher $CCN_{0.4}$ values (2900+/- 2800 cm^{-3}; Andreae, 2009), and spring (1997-2007, March-June) condensation nuclei (CN) concentrations for polluted continental air measured at Southern Great Plains Atmospheric Radiation Measurement (SGP-ARM) site in Oklahoma are a mean of 5,224 (± 783) CN cm^{-3} (Moyes et al. 2009), with a calculated 784-1,410 $CCN_{0.4}$ cm^{-3} using US $CCN_{0.4}$/CN ratios of 0.15-0.27 (Andreae, 2009). Though the following results apply a lower bound on clean, continental conditions, we also discuss implications for average observed clean conditions (200 CCN cm^{-3}) and polluted conditions (10^3 CCN cm^{-3}).

3 Results and discussion

3.1 Rupture mechanism and the dispersal of pollen and SPPs

The simulated monthly mean pollen emissions potential (grains m^{-2} d^{-1}; Figure 2a), or the maximum possible daily pollen emission flux prescribed to RegCM4 from Pollen Emissions for Climate Models (PECM1.0; Wozniak and Steiner 2017; Methods), shows the emergence of pollen in March in the southeastern and southwestern United States, increases throughout the continental United States with a maximum in the Western US in April, and maximum pollen potential in the Northern US in May. On the regional scale, the atmospheric SPP burden (SPPs m^{-2}) seasonally follows the spatial patterns of the pollen emission potential, with differences arising due to meteorological factors such as wind, RH and precipitation affecting SPP production and transport (Text S1). The atmospheric burden of SPPs in the SPP_LIT simulations reaches a seasonal peak in April (Figure 2b), with elevated (>1×10^9 SPP m^{-2}) SPP burden continuing through May in the Northeast; the SPP burden is otherwise quite high (>1×10^8 SPPs m^{-2}) throughout the season in most of the US. Unlike the pollen grains, which are more strongly affected by gravitational settling, SPPs accumulate in the atmosphere at the continental scale, leading to a SPP burden that is much greater than the pollen grain burden (10^8-10^9 SPPs m^{-2} versus 10^3-10^5 pollen grains m^{-2}; Fig. S1). The results are similar in SPP_HIGH (Fig. S2), though magnitudes are 1,000 times greater, scaling with n_{spg}.

Both surface and airborne rupture are promoted by elevated moisture (high RH or precipitation), but the latter also depends strongly on atmospheric pollen sources that are inhibited by moisture (Figure 1; Methods). Because of these inter-dependencies, the dominance of either surface or airborne production varies spatially. We define the Northeast (38-45ºN, 65-80ºW) and Mountain (35-42ºN, 100-116ºW) subregions (Fig. S3) as examples of wet and dry regions, respectively. In the Northeast, the mean surface RH

and precipitation vary between 60-100% and 0-22.5 mm d^{-1} respectively (Fig. 3b), and the average RH aloft often exceeds 60% (Fig 3c). Consequently, SPP surface emissions are consistently high throughout the season due to the abundant moisture and scale with pollen grain emissions and n_{spg} (i.e. SPP surface emissions are n_{spg} = 1,000 times greater than pollen emissions in SPP_LIT). Even though the average RH aloft is often greater than 60% (Figure 3c), the total atmospheric production of SPPs from airborne rupture is consistently about 1% of production from surface rupture throughout the season, likely due to moisture-inhibited pollen emissions and washout of airborne pollen by rain. This suggests that surface rupture is the dominant pathway for SPP formation in the Northeast.

Meanwhile, in the drier Mountain subregion, RH and precipitation are lower and more episodic (Figure 3e), causing the surface SPP emission flux to fluctuate over the season by about 1-3 orders of magnitude despite little variation in pollen emissions (Figure 3d). SPP surface emissions range between 10^6 to 10^9 SPPs m^{-2} d^{-1} in the beginning of the season (March, April) with late-season reductions (May, June) (Fig. 3d), and are often up to 10 times less than SPP surface emissions in the Northeast. Meanwhile, SPP airborne production is generally higher in the spring than the Northeast (e.g., by greater than a factor of 10 on day 137), which can be attributed to higher airborne pollen concentrations due to the lack of wet removal (Fig. S4), as well as sufficient moisture available aloft (Fig. 3f). There is also a seasonal change of the roles of surface versus airborne SPP production in the Mountain subregion. The surface rupture mechanism dominates over airborne rupture by about a factor of 10 in the beginning of the season, when conditions are more humid near the surface. Around day 120 (April 30), surface and airborne rupture production rates are similar due to decreasing surface humidity, then airborne rupture exceeds surface emissions by a factor of 10 by the end of the season (day 165 – day 181) when early summer drying occurs in the subregion.

The resulting SPP concentrations aloft also differ between the Northeast and Mountain subregions, mainly because moisture is associated with precipitation rates and therefore wet removal processes. In the Northeast (Fig. 3c), washout from precipitation modulates the accumulation of SPPs over the season, with maximum SPP concentrations alternating from 10^6-10^7 SPPs m^{-3} (1-10 cm^{-3}) in the near-surface layers (up to 750 hPa) and comparably low concentrations aloft (above 750 hPa; 10^3-10^5 SPPs m^{-3}). In the Mountain subregion (Fig. 3f), minimal precipitation reduces washout, and SPPs accumulate to a steady ~10^7 SPPs m^{-3} up to 750 hPa throughout the season without modulation from rain (concentrations aloft are similar to the Northeast). The spatiotemporal patterns of SPPs in the SPP_HIGH ensemble are similar to those in SPP_LIT (Fig. S5), except with magnitudes of 10^6-10^9 SPPs m^{-3} (1-1,000 cm^{-3}), proportional to the difference in n_{spg} (from 1,000 to 1×10^6 SPPs $grain^{-1}$).

3.2 Suppression of precipitation by SPPs

Simulated baseline accumulated precipitation shows a west-to-east gradient in the spring to summer transition, with light precipitation in the intermountain West (<100mm), moderate precipitation (100-400 mm) in the southern, southeastern and northwestern US, and heavier (400+ mm) precipitation in the region extending from the northern border of Texas through the eastern Great Lakes into the Northeast (Fig. 4a). To investigate the impact of SPPs as CCN on precipitation, we compare the two ensemble simulations, SPP_LIT and SPP_HIGH, with the BASE simulations. For SPP_LIT based on a literature-derived value of n_{spg}, the seasonal average CCN burden increases by a maximum of about 0.04-0.05% (Figure 4d) associated with a domain-average change of precipitation over land of +0.06%, likely due to residual model internal variability (see methods in SI). For this ensemble there is little change in seasonal precipitation (absolute value <5%) with no apparent spatial pattern (Figure 4b). However, in the SPP_HIGH simulation the CCN burden increases by 5-20% throughout the continental US (Figure 4e), and precipitation is reduced by 32% averaged over the continental US (Figure 4c). The greatest reductions occur in parts of the dry western US where changes are up to 100%. In the Southeast, precipitation is reduced up to 30%, while in the Midwest and Northeast, where baseline precipitation is at its maximum, precipitation is reduced by 30 to 55%.

In addition to the reductions in the seasonal accumulated precipitation in SPP_HIGH, daily precipitation intensity shifts from heavier to lighter magnitudes. In the Northeast subregion, there is about a 1% reduction of light precipitation (<1 mm d^{-1}), a 5% reduction in moderate precipitation (5-25 mm d^{-1}) and a <1% reduction in heavy precipitation (>25 mm d^{-1}), while very light (0.001-5 mm d^{-1}) precipitation increases by 7%, respectively. The number of dry days (not shown) increases by 26% for this subregion. Similar results occur for the Mountain subregion, where light and moderate precipitation events decrease by 5% and <1% while very light precipitation increases by 6% and the number of dry days increases by 8%. No heavy precipitation events occurred in the Mountain subregion in either the baseline or the SPP_HIGH simulations. Changes in the distribution for SPP_LIT are small (<0.1%), although they do show a 1% increase in dry days for the Northeast and a small increase (0.15%) for the Mountains. These results provide evidence that SPPs could impact precipitation intensity as well as the seasonal mean in clean CCN conditions, depending on how productive the pollen rupture process is. Though $n_{spg} = 10^6$ SPPs per grain is conservatively rounded to the nearest million from 3.06×10^6 SPPs per grain (Text S1), it may still be an overestimate. Background CCN concentrations also affect these results. In simulations with 200 CCN cm^{-3}, seasonal precipitation is reduced by 20% averaged over the domain, whereas in simulations of polluted atmospheres (10^3 CCN cm^{-3} background), it is a 2% reduction.

4 Conclusions

Our results provide the first assessment of the role of SPPs on regional

precipitation and climate. Additional laboratory experiments and field observations would provide important constraints to the model simulations. Although our representation of pollen rupture is supported by laboratory experiments (Taylor et al. 2002; Taylor et al. 2004; Grote et al. 2001; Grote et al. 2003), this details of this mechanism (e.g. humidity thresholds) have only been studied for grasses and a few tree genera. Quantifying rupture as a specific function of atmospheric parameters and more rigorous constraints on n_{spg} would greatly improve model simulations and bound the impact of SPP on precipitation. Also, new instrumental methodologies provide promise to evaluate SPP simulations with observations, such as the recent calibration of UV-induced fluorescence for identifying bioaerosol classes such as pollen (Hernandez et al., 2016). Finally, including other important precipitation processes like pollen grains as IN and giant CCN could enhance rain and compete with the suppression by SPPs, and this could more comprehensively account for the total impact of pollen on precipitation. Notwithstanding pollen alone, including the CCN and IN impacts of other bioaerosols may also influence the simulation of precipitation (Després et al., 2012; Morris et al., 2014), and we do not include those effects here.

These results can also inform allergenic and respiratory risk due to pollen. Typically, risk is assessed using pollen grain counts, yet pollen allergens have been detected in ambient measurements of particles smaller than pollen grains (Buters et al., 2010; Galan et al., 2013). It has been postulated that direct measurements of specific allergens in fine and coarse particulate rather than pollen grains may correlate better with observed allergic symptoms (Bastl et al., 2016). These simulations of the formation and burden of SPPs could improve estimates of allergy risk by predicting the distribution of pollen fragments that may cause allergy, both in the present-day and under future climate regimes.

Acknowledgements
This work was support by National Science Foundation grant AGS 0952659 to A.L.S.

Simulation data and model code is available at the URL https://deepblue.lib.umich.edu/data/concern/generic_works/nz806044h?locale=en, or upon direct request from M.C.W.

M.C.W. developed the rupture model, led the ensemble simulations and analysis, and wrote the paper. F.S. implemented the modifications to moisture parameterizations in RegCM4, guided the implementation of SPP as CCN as well as the simulation analysis, and commented on the paper. A.L.S. conceived of the project, guided the implementation and analysis, and edited the paper.

The authors declare no competing interests.

References

Albrecht, B. A. (1989). Aerosols, cloud microphysics, and fractional cloudiness. *Science*, *245*(4923), 1227.

Andreae, M. O. (2009). Correlation between cloud condensation nuclei concentration and aerosol optical thickness in remote and polluted regions. *Atmospheric Chemistry and Physics*, *9*(2), 543–556. http://doi.org/10.5194/acp-9-543-2009

Ariya, P. a., Sun, J., Eltouny, N. a., Hudson, E. D., Hayes, C. T., & Kos, G. (2009). *Physical and chemical characterization of bioaerosols – Implications for nucleation processes*. *International Reviews in Physical Chemistry* (Vol. 28). http://doi.org/10.1080/01442350802597438

Bastl, K., Kmenta, M., Pessi, A. M., Prank, M., Saarto, A., Sofiev, M., … Berger, U. (2016). First comparison of symptom data with allergen content (Bet v 1 and Phl p 5 measurements) and pollen data from four European regions during 2009-2011. *Science of the Total Environment*, *548–549*, 229–235. http://doi.org/10.1016/j.scitotenv.2016.01.014

Boucher, O., Randall, D., Artaxo, P., Bretherton, C., Feingold, G., Forster, P., … Zhang, X. Y. (2013). 7. Clouds and Aerosols. *Climate Change 2013: The Physical Science Basis. Contribution of Working Group I to the Fifth Assessment Report of the Intergovernmental Panel on Climate Change*, 571–657. http://doi.org/10.1017/CBO9781107415324.016

Buters, J. T. M., Weichenmeier, I., Ochs, S., Pusch, G., Kreyling, W., Boere, A. J. F., … Behrendt, H. (2010). The allergen Bet v 1 in fractions of ambient air deviates from birch pollen counts. *Allergy: European Journal of Allergy and Clinical Immunology*, *65*(7), 850–858. http://doi.org/10.1111/j.1398-9995.2009.02286.x

Carslaw, K. S., Gordon, H., Hamilton, D. S., Johnson, J. S., Regayre, L. A., Yoshioka, M., & Pringle, K. J. (2017). Aerosols in the Pre-industrial Atmosphere. *Curr Clim Change Rep*, *3*, 1–15. Retrieved from https://link.springer.com/content/pdf/10.1007%2Fs40641-017-0061-2.pdf

Carslaw, K. S., Lee, L. A., Reddington, C. L., Pringle, K. J., Rap, A., Forster, P. M., … Pierce, J. R. (2013). Large contribution of natural aerosols to uncertainty in indirect forcing. *Nature*, *503*(7474), 67–71. http://doi.org/10.1038/nature12674

Davis, M. B., & Brubaker, L. B. (1973). Differential Sedimentation of Pollen Grains in Lakes. *Limnology and Oceanography*, *18*(4), 635–646. http://doi.org/10.4319/lo.1973.18.4.0635

Dee, D. P., Uppala, S. M., Simmons, A. J., Berrisford, P., Poli, P., Kobayashi, S., … Rosnay, de P. (2011). The ERA-Interim reanalysis: configuration and performance of the data assimilation system. *Quarterly Journal of the Royal Meteorological Society Q. J. R. Meteorol. Soc*, *137*, 553–597. http://doi.org/10.1002/qj.828

Dengate, H. N., Baruch, D. W., & Meredith, P. (1978). The Density of Wheat Starch Granules: A Tracer Dilution Procedure for Determining the Density of an Immiscible Dispersed Phase. *Starch*, *30*(3), 80–84. Retrieved from https://onlinelibrary.wiley.com/doi/pdf/10.1002/star.19780300304

Despres, V. R., Alex Huffman, J., Burrows, S. M., Hoose, C., Safatov, A. S., Buryak, G., … Jaenicke, R. (2012). Primary biological aerosol particles in the atmosphere: A review. *Tellus, Series B: Chemical and Physical Meteorology*. http://doi.org/10.3402/tellusb.v64i0.15598

Diehl, K., Quick, C., Matthias-Maser, S., Mitra, S. K., & Jaenicke, R. (2001). The ice nucleating ability of pollen Part I: Laboratory studies in deposition and condensation freezing modes. *Atmospheric Research*, *58*, 75–87. Retrieved from www.elsevier.comrlocateratmos

Fischer, H., Polikarpov, I., & Craievich, A. F. (2004). Average protein density is a molecular-weight-dependent function. *Protein Science*, *13*(10), 2825–2828. http://doi.org/10.1110/ps.04688204

Fitzgerald, J. W. (1973). Dependence of the Supersaturation Spectrum of CCN on Aerosol Size Distribution and Composition. *Journal of the Atmospheric Sciences*, *30*, 628–634. Retrieved from https://journals.ametsoc.org/doi/pdf/10.1175/1520-0469%281973%29030%3C0628%3ADOTSSO%3E2.0.CO%3B2

Galan, C., Antunes, C., Brandao, R., Torres, C., Garcia-Mozo, H., Caeiro, E., … Buters, J. T. M. (2013). Airborne olive pollen counts are not representative of exposure to the major olive allergen Ole e 1. *Allergy: European Journal of Allergy and Clinical Immunology*, *68*(6), 809–812. http://doi.org/10.1111/all.12144

Giorgi, F. (1989). Two-dimensional simulations of possible mesoscale effects of nuclear war fires: 1. Model description. *Journal of Geophysical Research*, *94*(D1), 1127. http://doi.org/10.1029/JD094iD01p01127

Giorgi, F., & Bi, X. (2000). A study of internal variability of a regional climate model. *J. Geophys. Res.*, *105*(D24), 29503–29522. http://doi.org/10.1029/2000JD900269

Giorgi, F., & Chameides, W. L. (1986). Rainout lifetimes of highly soluble aerosols and gases as inferred from simulations with a general circulation model. *Journal of Geophysical Research*, *91*(D13), 14367. http://doi.org/10.1029/JD091iD13p14367

Giorgi, F., Coppola, E., Solmon, F., Mariotti, L., Sylla, M. B., Bi, X., … Brankovic, C. (2012). RegCM4: Model description and preliminary tests over multiple CORDEX domains. *Climate Research*, *52*(1), 7–29. http://doi.org/10.3354/cr01018

Grell, G. A., Dudhia, J., & Stauffer, D. R. (1994). A description of the Fifth-generation Penn State/NCAR Mesoscale Model (MM5). *NCAR Technical Note NCAR/TN-398+STR*, (December), 121. http://doi.org/10.5065/D60Z716B

Griffiths, P. T., Borlace, J. S., Gallimore, P. J., Kalberer, M., Herzog, M., & Pope, F. D. (2012). Hygroscopic growth and cloud activation of pollen: A laboratory and modelling study. *Atmospheric Science Letters*, *13*(4), 289–295.

http://doi.org/10.1002/asl.397
Grote, M., Valenta, R., & Reichelt, R. (2003). Abortive pollen germination: A mechanism of allergen release in birch, alder, and hazel revealed by immunogold electron microscopy. *Journal of Allergy and Clinical Immunology*, *111*(5), 1017–1023. http://doi.org/10.1067/mai.2003.1452
Grote, M., Vrtala, S., Niederberger, V., Wiermann, R., Valenta, R., & Reichelt, R. (2001). Release of allergen-bearing cytoplasm from hydrated pollen: A mechanism common to a variety of grass (poaceae) species revealed by electron microscopy. *Journal of Allergy and Clinical Immunology*, *108*(1), 109–115. http://doi.org/10.1067/mai.2001.116431
Hernandez, M., Perring, A. E., Mccabe, K., Kok, G., Granger, G., & Baumgardner, D. (2016). Chamber catalogues of optical and fluorescent signatures distinguish bioaerosol classes. *Atmos. Meas. Tech*, *9*, 3283–3292. http://doi.org/10.5194/amt-9-3283-2016
Jones, A., Roberts, D. L., & Wood, J. (2001). Indirect sulphate aerosol forcing in a climate model with an interactive sulphur cycle. *Europe*, *106*(D17), 20293–20310.
Lee, H., Yum, S. S., & Shim, S. (2016). Implementation of a new empirical relationship between aerosol and cloud droplet concentrations in a climate model. *Climate Research*, *70*(1), 57–76. http://doi.org/10.3354/cr01415
Liu, L., Solmon, F., Vautard, R., Hamaoui-laguel, L., Torma, C. Z., & Giorgi, F. (2016). Ragweed pollen production and dispersion modelling within a regional climate system , calibration and application over Europe, 2769–2786. http://doi.org/10.5194/bg-13-2769-2016
Liu, Y., Daum, P. H., & McGraw, R. (2004). An analytical expression for predicting the critical radius in the autoconversion parameterization. *Geophysical Research Letters*, *vol.31*, *no*(6), 4 pp. http://doi.org/10.1029/2003GL019117
Marousis, S. N., & Saravacos, G. . (1990). Density and Porosity in Drying Starch Materials. *Journal of Food Science*, *55*(5), 1367. Retrieved from https://onlinelibrary.wiley.com/doi/pdf/10.1111/j.1365-2621.1990.tb03939.x
Mlawer, E. J., Taubman, S. J., Brown, P. D., Iacono, M. J., & Clough, S. A. (1997). Radiative transfer for inhomogeneous atmospheres: RRTM, a validated correlated-k model for the longwave. *Journal of Geophysical Research*, *102*(D14), 16663–16682. http://doi.org/10.1029/97JD00237
Morris, C. E., Conen, F., Alex Huffman, J., Phillips, V., Pöschl, U., & Sands, D. C. (2014). Bioprecipitation: a feedback cycle linking earth history, ecosystem dynamics and land use through biological ice nucleators in the atmosphere. *Global Change Biology*, *20*(2), 341–51. http://doi.org/10.1111/gcb.12447
Moyes, A., Sedlacek, A., Behrens, B., Kuang, C., Salwen, C., Hageman, D., Andrews, E., Senum, G., Uin, J., Dubey, M., Boyer, M., Smith, S., Springston, S., & Watson, T. (2009). Aerosol Observing System (NOAAAOSAVG). Atmospheric Radiation

Measurement (ARM) Climate Research Facility. doi: 10.5439/1025260
O'Brien, T. A., Sloan, L. C., & Snyder, M. A. (2011). Can ensembles of regional climate model simulations improve results from sensitivity studies? *Climate Dynamics*, *37*(5), 1111–1118. http://doi.org/10.1007/s00382-010-0900-5
Oleson, K., Lawrence, D., Bonan, G., Flanner, M., & E., K. (2010). Technical Description of version 4.0 of the Community Land Model (CLM). *NCAR Technical Note NCAR/TN-478+STR*, 257.
Pal, J. S., Small, E. E., & Eltahir, E. A. B. (2000). Simulation of regional-scale water and energy budgets: Representation of subgrid cloud and precipitation processes within RegCM. *Journal of Geophysical Research: Atmospheres*, *105*(D24), 29579–29594. http://doi.org/10.1029/2000JD900415
Perring, A. E., Schwarz, J. P., Baumgardner, D., Hernandez, M. T., Spracklen, D. V, Heald, C. L., … Fahey, D. W. (2014). Airborne observations of regional variation in fluorescent aerosol across the United States, 1153–1170. http://doi.org/10.1002/2014JD022495.Received
Pope, F. D. (2010). Pollen grains are efficient cloud condensation nuclei. *Environmental Research Letters*, *5*(4), 44015. http://doi.org/10.1088/1748-9326/5/4/044015
Qian, Y., Giorgi, F., Huang, Y., Chameides, W., & Luo, C. (2001). Regional simulation of anthropogenic sulfur over East Asia and its sensitivity to model parameters. *Tellus, Series B: Chemical and Physical Meteorology*, *53*(2), 171–191. http://doi.org/10.1034/j.1600-0889.2001.d01-14.x
Rathnayake, C. M., Metwali, N., Jayarathne, T., Kettler, J., Huang, Y., Thorne, P. S., … Stone, E. A. (2017). Influence of rain on the abundance of bioaerosols in fine and coarse particles. *Atmospheric Chemistry and Physics*, *17*(3), 2459–2475. http://doi.org/10.5194/acp-17-2459-2017
Regayre, L. A., Pringle, K. J., Booth, B. B. B., Lee, L. A., Mann, G. W., Browse, J., … Carslaw, K. S. (2014). Uncertainty in the magnitude of aerosol-cloud radiative forcing over recent decades. *Geophysical Research Letters*, *41*(24), 9040–9049. http://doi.org/10.1002/2014GL062029
Salwen, C., Andrews, E., Senum, G., Uin, J., & Springston, S. (2010). Cloud Condensation Nuclei Particle Counter (AOSCCN100). Atmospheric Radiation Measurement (ARM) Climate Research Facility. doi: 10.5439/1025150
Samy, S., Mazzoleni, L. R., Mishra, S., Zielinska, B., & Hallar, A. G. (2010). Water-soluble organic compounds at a mountain-top site in Colorado, USA. *Atmospheric Environment*, *44*(13), 1663–1671. http://doi.org/10.1016/j.atmosenv.2010.01.033
Smith, T. M., Reynolds, R. W., Peterson, T. C., & Lawrimore, J. (2008). Improvements to NOAA's historical merged land-ocean surface temperature analysis (1880-2006). *Journal of Climate*, *21*(10), 2283–2296. http://doi.org/10.1175/2007JCLI2100.1
Sofiev, M., Siljamo, P., Ranta, H., Linkosalo, T., Jaeger, S., Rasmussen, a., … Kukkonen, J. (2013). A numerical model of birch pollen emission and dispersion in

the atmosphere. Description of the emission module. *International Journal of Biometeorology*, *57*(1), 45–58. http://doi.org/10.1007/s00484-012-0532-z

Solmon, F., Giorgi, F., & Liousse, C. (2006). Aerosol modelling for regional climate studies: Application to anthropogenic particles and evaluation over a European/African domain. *Tellus, Series B: Chemical and Physical Meteorology*, *58*(1), 51–72. http://doi.org/10.1111/j.1600-0889.2005.00155.x

Steiner, A. L., Brooks, S. D., Deng, C., Thornton, D. C. O., Pendleton, M. W., & Bryant, V. (2015). Pollen as atmospheric cloud condensation nuclei. *Geophysical Research Letters*, *42*(9), 3596–3602. http://doi.org/10.1002/2015GL064060

Stevens, B., & Feingold, G. (2009). Untangling aerosol effects on clouds and precipitation in a buffered system. *Nature*, *461*(7264), 607–613. http://doi.org/10.1038/nature08281

Stocker, T. F., Dahe, Q., Plattner, G.-K., Alexander, L. V., Allen, S. K., Bindoff, N. L., … Xie, S.-P. (2013). Technical Summary. *Climate Change 2013: The Physical Science Basis. Contribution of Working Group I to the Fifth Assessment Report of the Intergovernmental Panel on Climate Change*, 33–115. http://doi.org/10.1017/CBO9781107415324.005

Sun, J., & Ariya, P. (2006). Atmospheric organic and bio-aerosols as cloud condensation nuclei (CCN): A review. *Atmospheric Environment*, *40*(5), 795–820. http://doi.org/10.1016/j.atmosenv.2005.05.052

Sundqvist, H., Berge, E., & Kristjánsson, J. E. (1989). Condensation and Cloud Parameterization Studies with a Mesoscale Numerical Weather Prediction Model. *Monthly Weather Review*. http://doi.org/10.1175/1520-0493(1989)117<1641:CACPSW>2.0.CO;2

Suphioglu, C., Singh, M. B., Taylor, P., Knox, R. B., Bellomo, R., Holmes, P., & Puy, R. (1992). Mechanism of grass-pollen-induced asthma. *The Lancet*, *339*(8793), 569–572. http://doi.org/10.1016/0140-6736(92)90864-Y

Taylor, P. E., Flagan, R. C., Miguel, A. G., Valenta, R., & Glovsky, M. M. (2004). Birch pollen rupture and the release of aerosols of respirable allergens. *Clinical and Experimental Allergy*, *34*(10), 1591–1596. http://doi.org/10.1111/j.1365-2222.2004.02078.x

Taylor, P. E., Flagan, R. C., Valenta, R., & Glovsky, M. M. (2002). Release of allergens as respirable aerosols: A link between grass pollen and asthma. *Journal of Allergy and Clinical Immunology*, *109*(1), 51–56. http://doi.org/10.1067/mai.2002.120759

Tiedtke, M. (1989). A comprehensive mass flux scheme for cumulus parameterization in large-scale models. *Mon. Weather Rev.* http://doi.org/10.1175/1520-0493(1989)117<1779:ACMFSF>2.0.CO;2

Tiedtke, M. (1993). Representation of Clouds in Large-Scale Models. *Monthly Weather Review*, *121*(11), 3040–3061. http://doi.org/10.1175/1520-0493(1993)121<3040:ROCILS>2.0.CO;2

Twomey, S. (1991). Aerosols, clouds and radiation. *Atmospheric Environment. Part A. General Topics*, *25*(11), 2435–2442. http://doi.org/10.1016/0960-1686(91)90159-5

Visez, N., Chassard, G., Azarkan, N., Naas, O., Sénéchal, H., Sutra, J.-P., … Choël, M. (2015). Wind-induced mechanical rupture of birch pollen: Potential implications for allergen dispersal. *Journal of Aerosol Science*, *89*, 77–84. http://doi.org/10.1016/j.jaerosci.2015.07.005

Williams, C. G., & Després, V. (2017). Northern Hemisphere forests at temperate and boreal latitudes are substantial pollen contributors to atmospheric bioaerosols. *Forest Ecology and Management*, *401*, 187–191. http://doi.org/10.1016/j.foreco.2017.06.040

Wozniak, M. C., & Steiner, A. L. (2017). A prognostic pollen emissions model for climate models (PECM1.0). *Geoscientific Model Development*, (June), 1–36. http://doi.org/10.5194/gmd-10-4105-2017

Zhang, L., Gong, S., Padro, J., & Barrie, L. (2001). A size-segregated particle dry deposition scheme for an atmospheric aerosol module. *Atmospheric Environment*, *35*, 549–560.

Figures

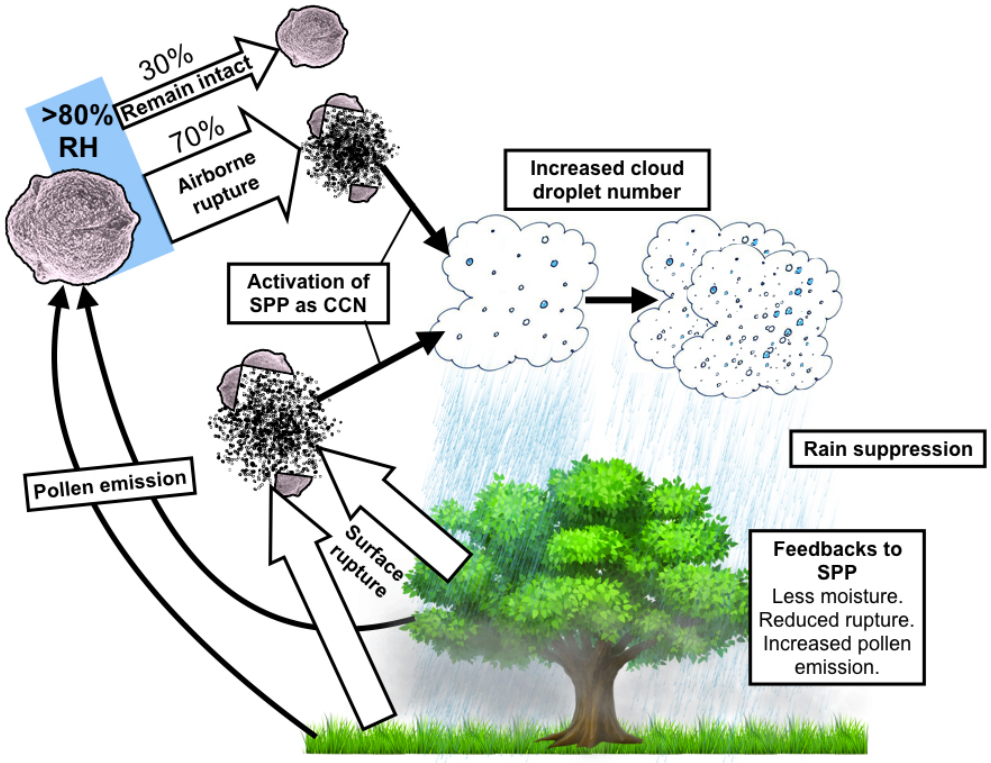

Figure 1. Conceptual diagram of pollen emissions, rupture, SPP production and impact on precipitation processes.

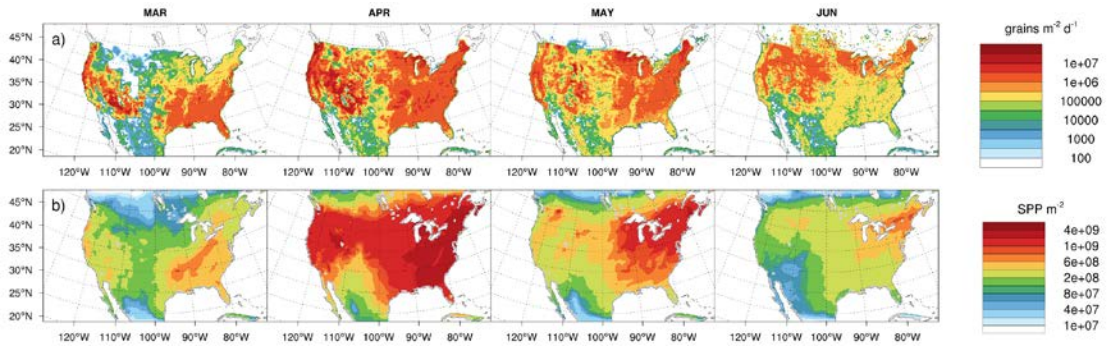

Figure 2. Simulated pollen emissions potential and SPP burden. Monthly mean **a)** pollen emission potential (grains m^{-2} d^{-1}) and **b)** SPP burden (SPPs m^{-2}) averaged over ten ensemble members (n_{spg} = 10^3 SPPs $grain^{-1}$, SPP_LIT) for the 2002 pollen season (March – June). In a second 10-member ensemble, SPP_HIGH (n_{spg} = 10^6 SPPs $grain^{-1}$), the spatial burden has the

same distribution as (b), but magnitudes are 1,000 times higher (Fig. S2).

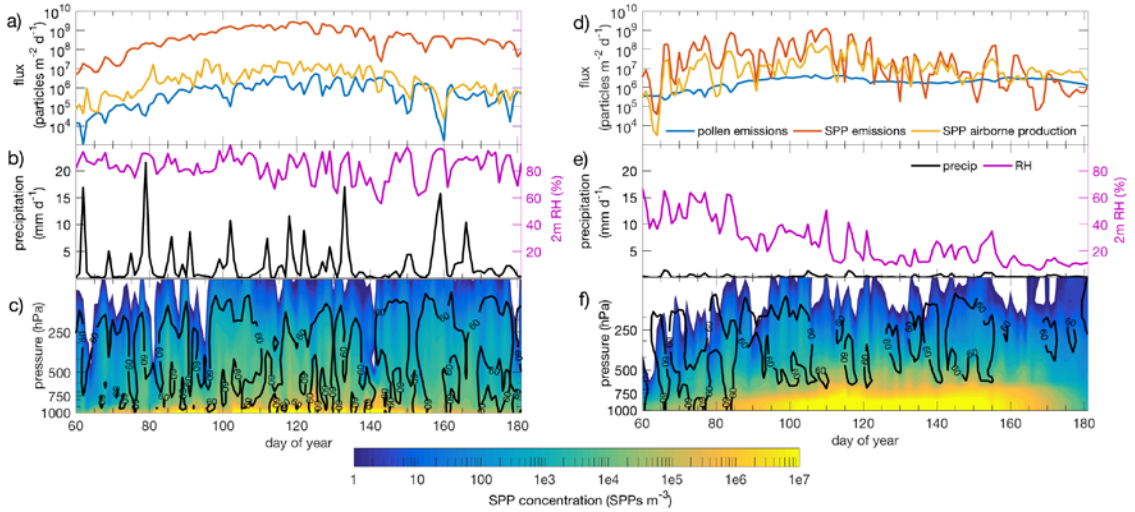

Figure 3. Regional evolution of the mean pollen and SPP source fluxes over the Northeast (a,b,c) and Mountain (d,e,f) subregions (Figure S3). Panels: **a,d)** Ensemble-averaged time series of mean daily pollen emissions (particles m^{-2} d^{-1}; blue), SPP emissions from surface rupture (particles m^{-2} d^{-1}; red), and SPP production from airborne rupture (particles m^{-2} d^{-1}; yellow). **b,e)** Ensemble-averaged time series of mean daily precipitation (mm d^{-1}; black) and 2 meter RH (%; magenta). **c,f)** Vertical profile of mean SPP concentration (SPPs m^{-3}; color contour) and RH (black contour = 60%).

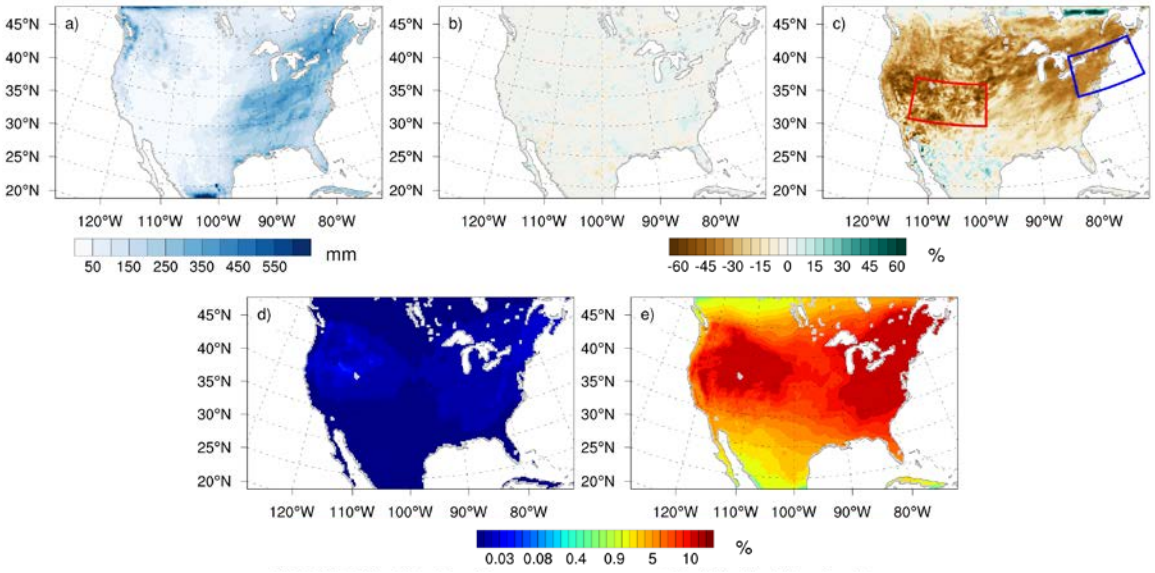

Figure 4. Precipitation and CCN changes driven by SPP.
a) Seasonal (March-June 2002) accumulated surface precipitation for BASE (mm), **b)** change of

seasonal precipitation from BASE to SPP_LIT (%), and **c)** change of seasonal precipitation from BASE to SPP_HIGH (boxes highlight the Northeast and Mountain subregions, Fig. S3). **d)** Change (%) of seasonal mean (Mar-June) CCN burden (CCN m^{-2}) from BASE to SPP_LIT, **e)** same as d) but from BASE to SPP_HIGH**.**

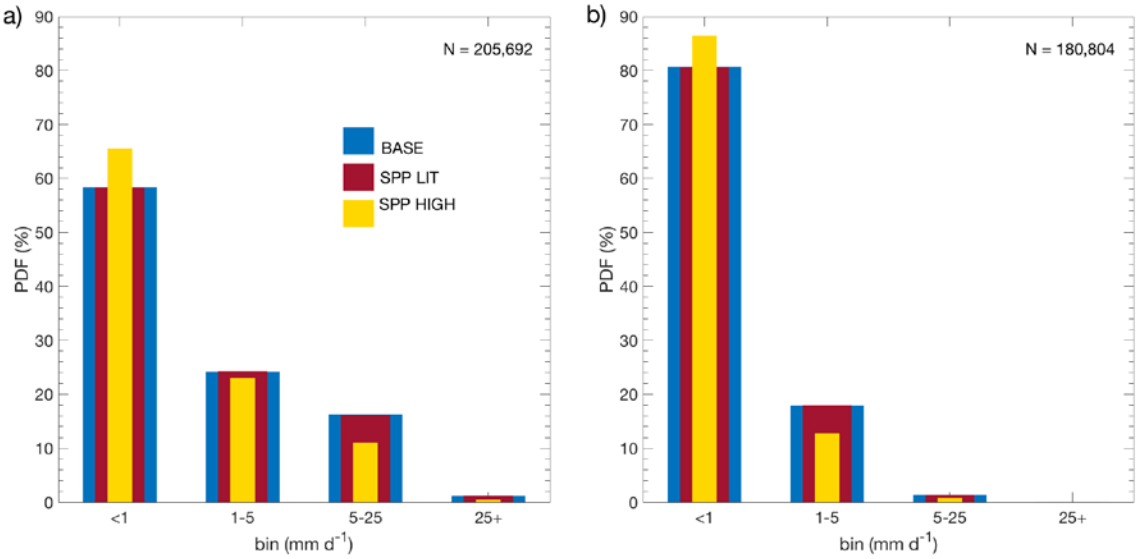

Figure 5. Daily precipitation intensity probability distribution functions (%) for Northeast and Mountain subregions throughout 2002 pollen season (day 60 – 181; March - June). Bins represent zero to very light (<1 mm d^{-1}), light (1-5 mm d^{-1}), moderate (5-25 mm d^{-1}), and heavy (>25 mm d^{-1}) for **a)** all grid cells in the Northeast subregion (# grid points = 1,656) and **b)** all grid cells the Mountain subregion (# grid points = 1,482).

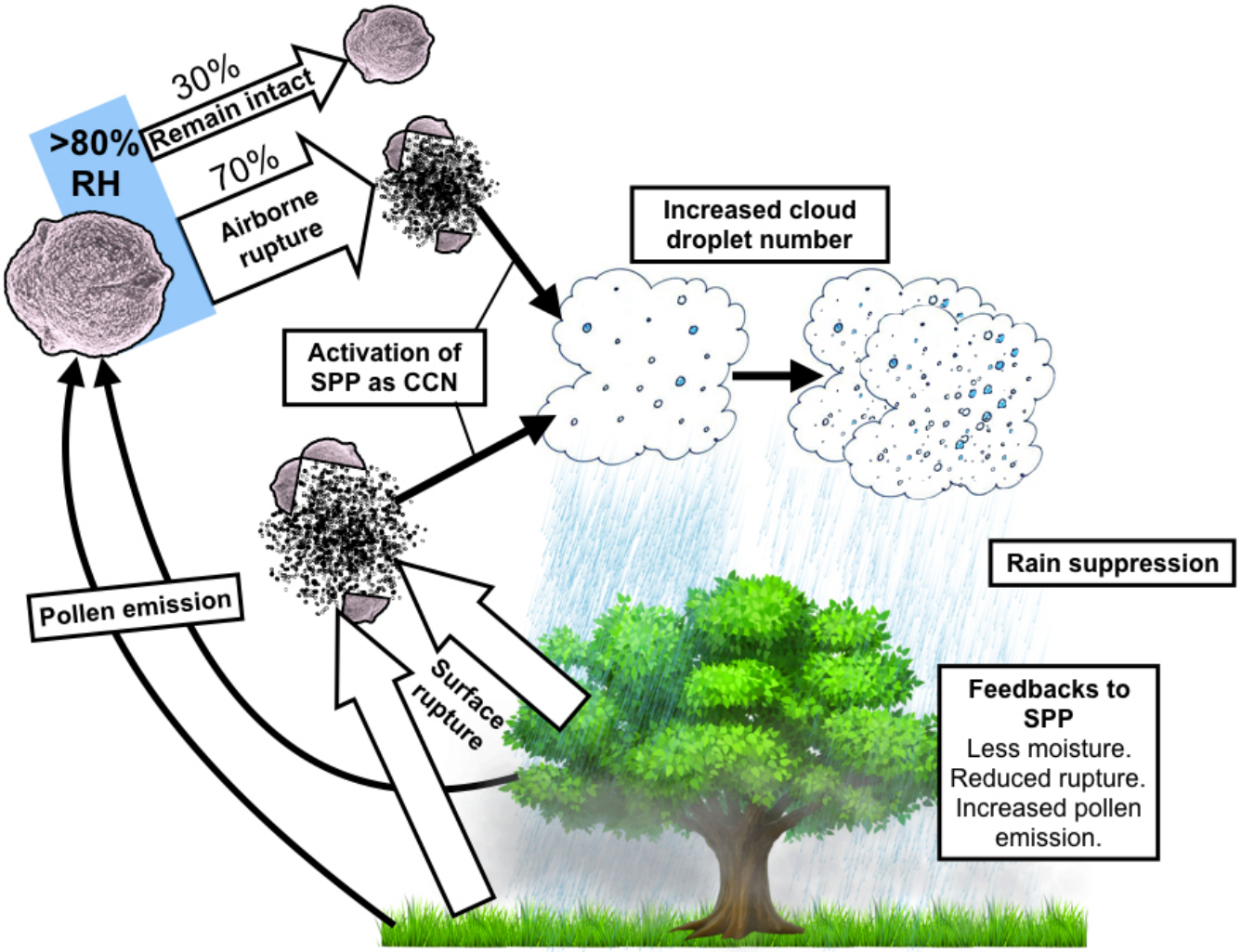

2018GL077692-f01-z-.jpg

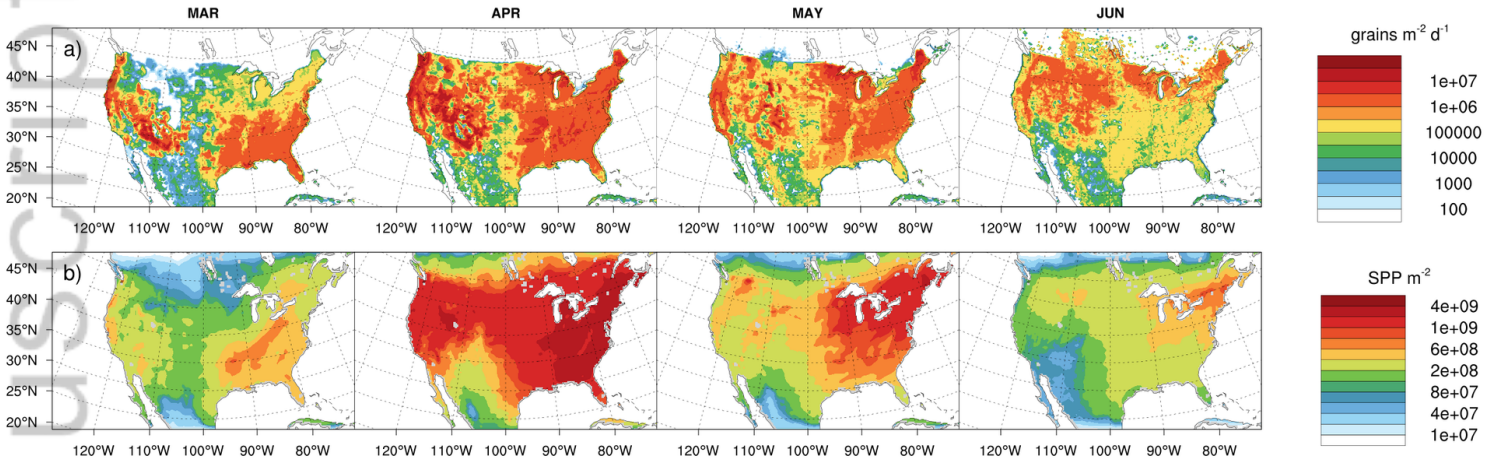

2018GL077692-f02-z-.png

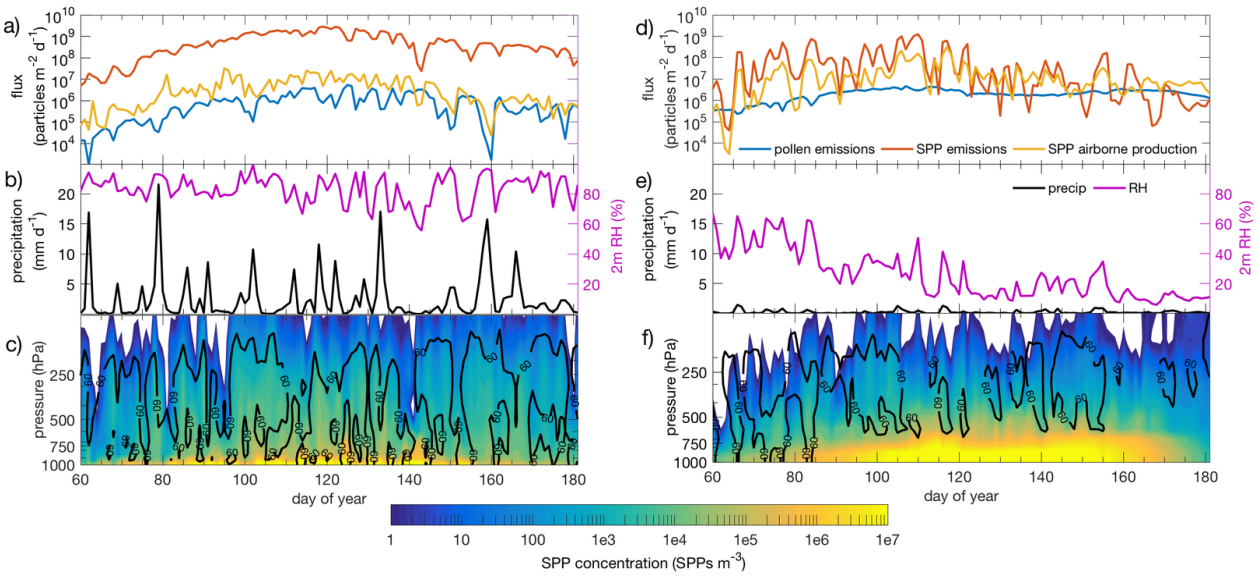

2018GL077692-f03-z-.png

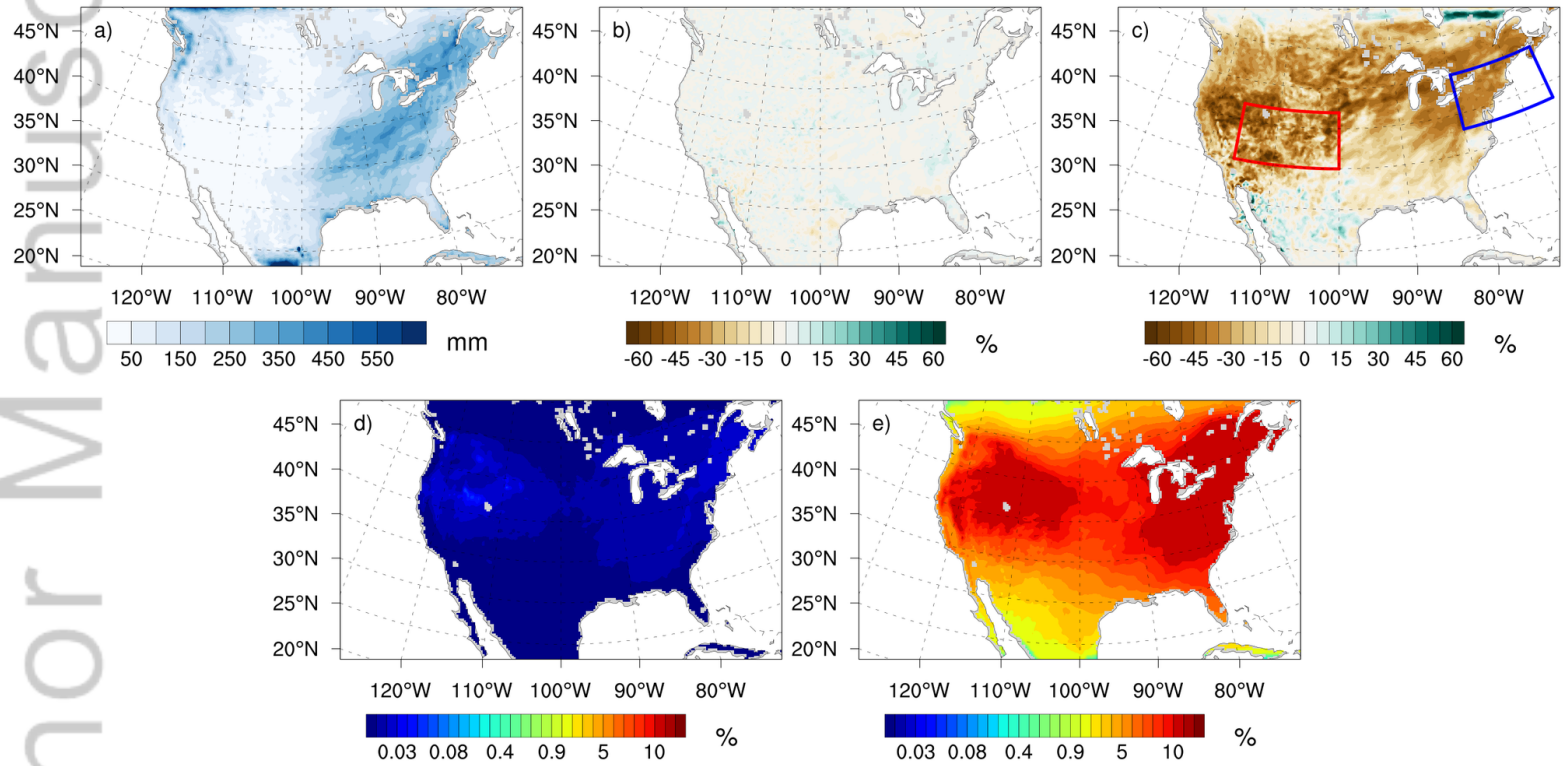

2018GL077692-f04-z-.png

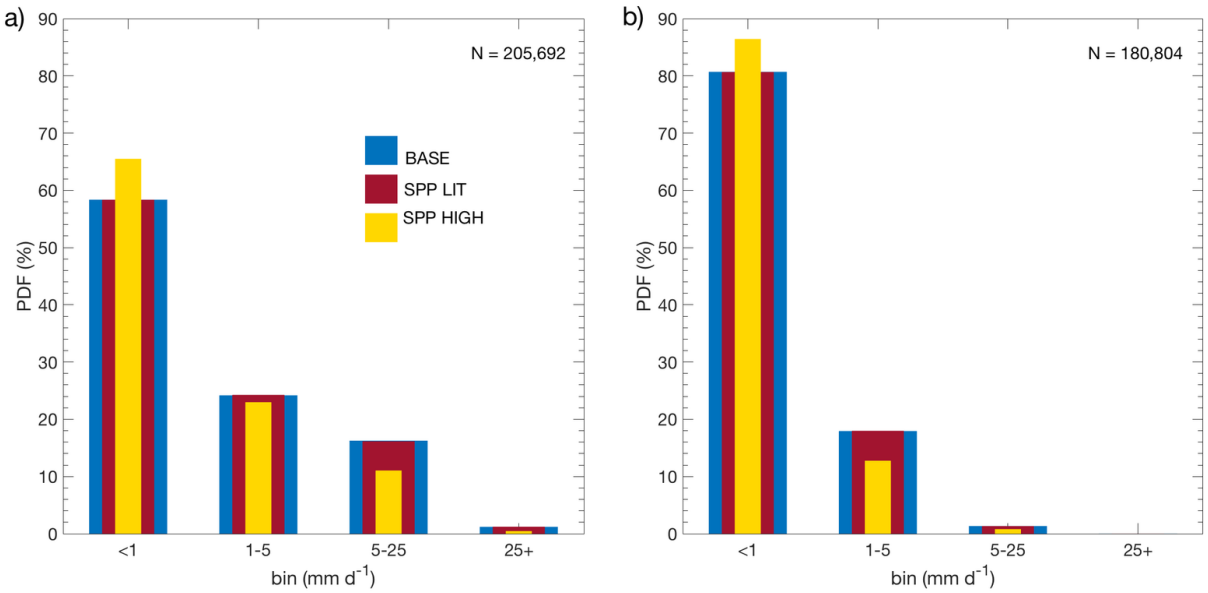

2018GL077692-f05-z-.png